Available online at www.sciencedirect.com
SCIENCE DIRECT®
Control Engineering Practice 12 (2004) 1531–1539
CONTROL ENGINEERING PRACTICE
www.elsevier.com/locate/conengprac

Adaptive tuning of a Kalman filter via fuzzy logic for an intelligent AUV navigation system

D. Loebis*, R. Sutton, J. Chudley, W. Naeem

Marine and Industrial Dynamic Analysis Research Group, School of Engineering, The University of Plymouth, Drake Circus, Plymouth PL4 8AA, UK

Received 17 August 2003; accepted 27 November 2003

Abstract

This paper describes the implementation of an intelligent navigation system, based on the integrated use of the global positioning system (GPS) and several inertial navigation system (INS) sensors, for autonomous underwater vehicle (AUV) applications. A simple Kalman filter (SKF) and an extended Kalman filter (EKF) are proposed to be used subsequently to fuse the data from the INS sensors and to integrate them with the GPS data. The paper highlights the use of fuzzy logic techniques to the adaptation of the initial statistical assumption of both the SKF and EKF caused by possible changes in sensor noise characteristics. This adaptive mechanism is considered to be necessary as the SKF and EKF can only maintain their stability and performance when the algorithms contain the true sensor noise characteristics. In addition, fault detection and signal recovery algorithms during the fusion process to enhance the reliability of the navigation systems are also discussed herein. The proposed algorithms are implemented to real experimental data obtained from a series of AUV trials conducted by running the low-cost *Hammerhead* AUV, developed by the University of Plymouth and Cranfield University.

Keywords: Autonomous underwater vehicles; Navigation; Sensor fusion; Kalman filters; Extended Kalman filters; Fuzzy logic

1. Introduction

The development of autonomous underwater vehicles (AUVs) for scientific, military and commercial purposes in applications such as ocean surveying (Størkersen, Kristensen, Indreeide, Seim, & Glancy, 1998), unexploded ordnance hunting (Wright et al., 1996) and cable tracking and inspection (Asakawa, Kojima, Kato, Matsumoto, & Kato, 2000) requires the corresponding development of navigation systems. Such systems are necessary to provide knowledge of vehicle position and attitude. The need for accuracy in such systems is paramount: erroneous position and attitude data can lead to a meaningless interpretation of the collected data or even to a catastrophic failure of an AUV.

A growing number of research groups around the world are developing integrated navigation systems utilising inertial navigation system (INS) and global positioning system (GPS) (Gade & Jalving, 1999; Grenon, An, Smith, & Healey, 2001; Yun et al., 1999). However, few of these works make explicit the essential need for fusion of several INS sensors that enable the users to maintain the accuracy or even to prevent a complete failure of this part of the navigation system, before being integrated with the GPS. Kinsey and Whitcomb (2003), e.g. use a switching mechanism to prevent a complete failure of the INS. Although simple to implement, the approach may not be appropriate to use to maintain a certain level of accuracy.

Several estimation methods have been used in the past for multisensor data fusion and integration purpose (Loebis, Sutton, & Chudley, 2002). To this end, simple/extended Kalman filter (SKF/EKF) and their variants have been popular methods in the past and interest in developing the algorithms has continued to the present day. However, a significant difficulty in designing a SKF/EKF can often be traced to incomplete a priori knowledge of the process covariance matrix (Q) and measurement noise covariance matrix (R). In most practical applications, these matrices are initially estimated or even unknown. The problem here is that the optimality of the estimation algorithm in the SKF/EKF

*Corresponding author. Tel.: +44-1752232633; fax: +44-1752232638.
E-mail address: d.loebis@plymouth.ac.uk (D. Loebis).

0967-0661/$ - see front matter © 2004 Elsevier Ltd. All rights reserved.
doi:10.1016/j.conengprac.2003.11.008

setting is closely connected to the quality of a priori information about the process and measurement noise (Mehra, 1970, 1971). It has been shown that insufficiently known a priori filter statistics can reduce the precision of the estimated filter states or introduces biases to their estimates. In addition, incorrect a priori information can lead to practical divergence of the filter (Fitzgerald, 1971). From the aforementioned, it may be argued that the conventional SKF/EKF with fixed R and/or Q should be replaced by an adaptive estimation formulation as discussed in the next section.

2. The adaptive tuning of Kalman filter algorithm

In the past few years, only a few publications in the area of adaptive Kalman filtering can be found in the literature. The two major approaches that have been proposed for adaptive Kalman filtering are multiple model adaptive estimation (MMAE) and innovation adaptive estimation (IAE). Although the implementation of these approaches are quite different, they both share the same concept of utilising new statistical information obtained from the innovation (or residual) sequence. In both cases, the innovation Inn_k at sample time k is the difference between the real measurement z_k, received by the filter and its estimated (predicted) value $\hat{z}_k$. The predicted measurement is the projection of the filter predicted states $\hat{x}_k^-$ onto the measurement space through the measurement design matrix H_k. Innovation represents additional information available to the filter as a result of the new measurement z_k. The occurrence of data with statistics different from the a priori information will first show up in the innovation vector. For this reason, the innovation sequence represents the information content in the new observation and is considered the most relevant source of information to the filter adaptation. Interested readers can refer to (Kailath, 1968a, b, 1970) for a more detailed discussion of the innovation sequence and its use in linear filter theory.

In the MMAE approach, a bank of Kalman filters runs in parallel (Magill, 1965; Hanlon & Maybeck, 2000) or with a gating algorithm (Chaer, Bishop, & Ghough, 1997) under a different model for the statistical filter information matrices, i.e. Q and R. In the IAE approach (Mehra, 1970, 1971), the Q and R matrices themselves are adapted as measurements evolve with time. In this paper, the IAE approach coupled with fuzzy logic techniques with membership functions designed using heuristic methods is used to adjust the R matrix of both the SKF and EKF. The proposed algorithms in this paper are implemented using a set of experimental data obtained from the *Hammerhead* AUV trials conducted in July 2003 at Roadford Reservoir, Devon, UK. Initial work using purely simulated data on the proposed algorithms can be found in Loebis, Sutton, and Chudley, 2003b and Loebis, Chudley, and Sutton, 2003a.

2.1. Fuzzy simple Kalman filter

In this section, an on-line innovation-based adaptive scheme of the SKF to adjust the R matrix employing the principles of fuzzy logic is presented. The fuzzy logic is chosen mainly because of its simplicity. This motivates the interest in the topic, as testified by related papers which have been appearing in the literature (Kobayashi, Cheok, Watanabe, & Muneka, 1998; Jetto, Longhi, & Vitali, 1999; Loebis et al., 2003a, b). The fuzzy logic simple Kalman filter (FSKF) proposed herein and fuzzy logic extended Kalman filter (FEKF) discussed in Section 4 are based on the IAE approach using a technique known as covariance matching (Mehra, 1970). The basic idea behind the technique is to make the actual value of the covariance of the innovation sequences match its theoretical value.

The actual covariance is defined as an approximation of the Inn_k sample covariance through averaging inside a moving estimation window of size M (Mohamed & Schwarz, 1999) which takes the following form:

$$\hat{C}_{Inn_k} = \frac{1}{M}\sum_{j=j_0}^{k} Inn_k\, Inn_k^T, \tag{1}$$

where $j_0 = k - M + 1$ is the first sample inside the estimation window. An empirical experiment is conducted to choose the window size M. From experimentation, it was found that a good size for the moving window in (1) is 15.

The theoretical covariance of the innovation sequence is defined as

$$S_k = H_k P_k^- H_k^T + R_k. \tag{2}$$

The logic of the adaptation algorithm using covariance matching technique can be qualitatively described as follows. If the actual covariance value $\hat{C}_{Inn_k}$ is observed, whose value is within the range predicted by theory S_k and the difference is very near to zero, this indicates that both covariances match almost perfectly and only a small change is needed to be made on the value of R. If the actual covariance is greater than its theoretical value, the value of R should be decreased. On the contrary, if $\hat{C}_{Inn_k}$ is less than S_k, the value of R should be increased. This adjustment mechanism lends itself very well to being dealt with using a fuzzy-logic approach based on rules of the kind:

$$\text{IF} < \textit{antecedent} > \text{THEN} < \textit{consequent} >, \tag{3}$$

where antecedent and consequent are of the form $\chi \in O_i$, $\kappa \in L_i$, $i = 1, 2, \ldots$, respectively, where χ and κ are the input and output variables, respectively, and O_i and L_i are the fuzzy sets.

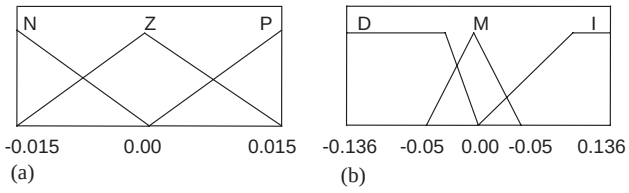

Fig. 1. Membership function of: (a) $delta_k$, and (b) ΔR_k.

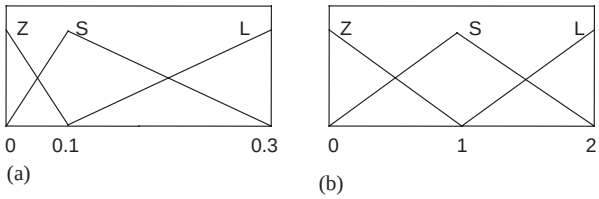

Fig. 2. Membership function of: (a) $|delta_k|$, and (b) R_k.

To implement the above covariance matching technique using the fuzzy logic approach, a new variable called $delta_k$, is defined to detect the discrepancy between $\hat{C}_{Inn_k}$ and S_k. It is important to note that in this particular application, $\hat{C}_{Inn_k}$ and S_k are constrained to be diagonal matrices. The following three fuzzy rules of the kind (3) are used:

$$\text{IF} < delta_k \cong 0 > \text{THEN} < R_k \text{ is unchanged} >, \quad (4)$$

$$\text{IF} < delta_k > 0 > \text{THEN} < R_k \text{ is decreased} >, \quad (5)$$

$$\text{IF} < delta_k < 0 > \text{THEN} < R_k \text{ is increased} >. \quad (6)$$

Thus R is adjusted according to

$$R_k = R_{k-1} + \Delta R_k, \quad (7)$$

where ΔR_k is added or subtracted from R at each instant of time. Here $delta_k$ is the input to the fuzzy inference system (FIS) and ΔR_k is the output.

On the basis of the above adaptation hypothesis, the FIS can be implemented using three fuzzy sets for $delta_k$; $N = Negative$, $Z = Zero$ and $P = Positive$. For ΔR_k the fuzzy sets are specified as $I = Increase$, $M = Maintain$ and $D = Decrease$. The membership functions of these fuzzy sets which are designed using a heuristic approach are shown in Fig. 1.

2.2. Sensor fault diagnostic and recovery algorithm

In addition to the adaptation procedure, the FSKF has been equipped with the sensor fault diagnostic and recovery algorithm as proposed by Escamilla-Ambrosio & Mort (2001). The basic idea behind this algorithm is that the amplitude of the actual value of the Inn_k and its theoretical value ($\sqrt{S_k}$) for a sensor without any fault must be around 1, but it increases abruptly if a transient or persistent fault is present in the measurement data. For this purpose a variable $InnC_k$is defined as

$$InnC_k = \frac{|Inn_k|}{\sqrt{S_k}}. \quad (8)$$

Thus, if the value of $InnC_k$ is greater or equal than a threshold (α) then a transient fault is declared and Inn_k is assigned a value of 0. If $InnC_k$ is still greater than α for an instant of time, the persistent fault is declared and Inn_k is assigned a value of $\sqrt{S_k}$ multiplied by a random number. From experimentation, it was found that the good value of α is 1.2.

Table 1
Fuzzy rule base FLO

$\|delta_k\|$	R_k		
	Z	S	L
Z	G	G	AV
S	G	AV	P
L	AV	P	P

2.3. Fuzzy logic observer

To monitor the performance of a FSKF, another FIS called the fuzzy logic observer (FLO) (Escamilla-Ambrosio & Mort, 2001) is used. The FLO assigns a weight or degree of confidence denoted as c_k, a number on the interval [0,1], to the FSKF state estimate. The FLO is implemented using two inputs: the values of $|delta_k|$ and R_k. The membership functions of these variables were found using a heuristic method that produced a non-symmetrical shape for $|delta_k|$ and a symmetrical shape for R_k are shown in Fig. 2.

The fuzzy labels for the membership functions: Z = Zero, S = Small and L = Large. Three fuzzy singletons are defined for the output c_k and are labelled as G = Good, AV = Average and P = Poor with values 1, 0.5 and 0, respectively. The basic heuristic hypothesis for the FLO is as follows: if the value of $|delta_k|$ is near to zero and the value of R_k is near to zero, then the FSKF works almost perfectly and the state estimate of the FSKF is assigned a weight near 1. On the contrary, if one or both of these values increases far from zero, it means that the FSKF performance is degrading and the FLO assigns a weight near 0. Table 1 gives the complete fuzzy rule base of each FLO.

3. Fusion of INS sensor data

In this section, the FSKF algorithm is applied to the linear heading model of the *Hammerhead* AUV. Fig. 3(a) shows the vehicle before leak testing and

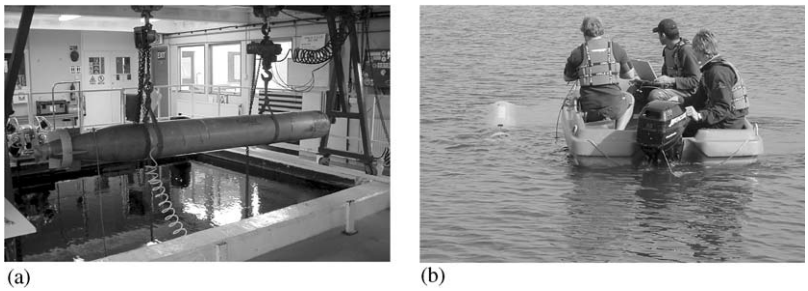

(a) (b)

Fig. 3. The *Hammerhead* AUV: (a) before leak testing and ballasting, and (b) during a system identification trial.

ballasting in the laboratory test tank and Fig. 3(b) shows the vehicle during a heading system identification trial. Inputs to the rudder of the vehicle are sent by the user from a laptop through an umbilical cable. Thus in reality it was travelling in a semi-autonomous model for that specific trial. The drag effect of the cable is considered to be negligible. An electronic compass and an inertial measurement unit (IMU) on board the vehicle are used to capture the corresponding responses.

The system matrix (A), input matrix (B), and output vector (H) of the linear discrete state space model (see Appendix A) obtained from the trial data are, respectively, $A = [0\ \ 1;\ \ -0.98312\ \ 1.9831]$, $B = [-0.0031961\ \ -0.0036115]$, $H = \begin{bmatrix} 1 & 0 \end{bmatrix}$, with the yaw and delayed-yaw as the component of the states.

This model is assumed to be sufficiently accurate to represent the dynamics of the vehicle, and for this reason, any output produced by the model after being excited by an input, can be considered as an actual output value. This assumption also motivates the use of the model output as a reference in measuring the performance of the FSKF algorithms.

To test the FSKF algorithms, real data obtained from the electronic compass and IMU (Fig. 5), as a response to the input shown in Fig. 4, are fused together with two sets of simulated data. To produce the simulated data, the noise in Figs. 6(a) and (b) are simply added to the electronic compass and IMU real data, respectively. A possible real-time scenario that can result in the noise with the characteristic shown in Fig. 6(a) is that the second electronic compass is located in close proximity to the propeller DC motor whose internal temperature increases with time and affects the sensor ambient temperature. A similar scenario can also be considered to occur when the second IMU is located in close proximity to the front hydroplane stepper motor whose initial internal temperature is high and settles down after sometime. This particular scenario can result in the noise characteristic as shown in Fig. 6(b). The initial condition of the states are $\begin{bmatrix} 0 & 0 \end{bmatrix}^T$, $P_0 = 0.01I_2$ (see Appendix A) and $Q = \mathrm{diag}(0, 0.1725 \times 10^{-7})$. The actual value of R for each sensor is assumed unknown, but its initial value is selected as 1. Simulation results are shown in the next section.

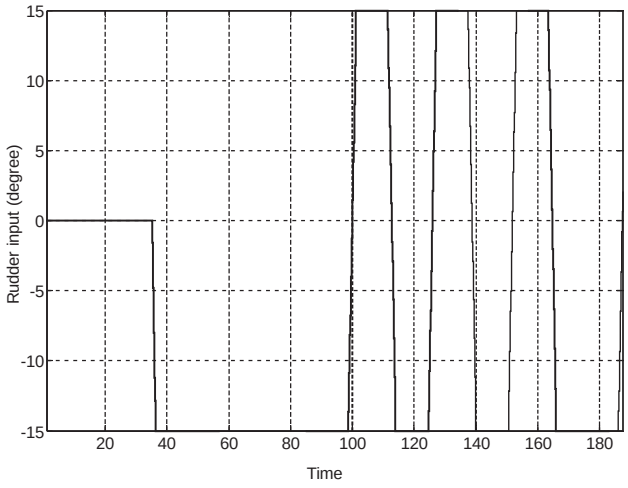

Fig. 4. Input rudder.

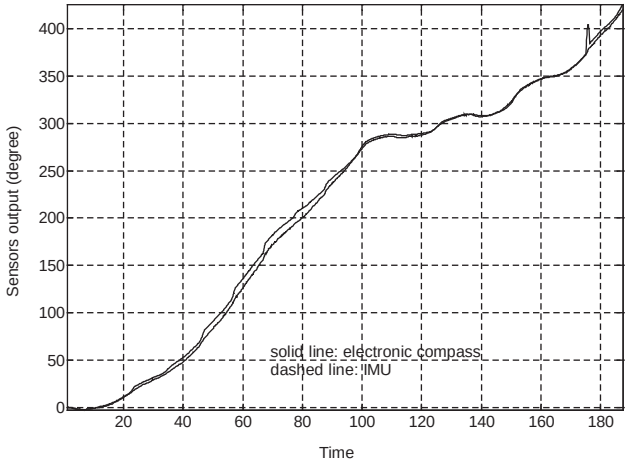

Fig. 5. Real electronic compass and IMU output.

3.1. Simulation result

Figs. 7 and 8 are the simulation results showing the response of the *Hammerhead* AUV observed by electronic compass and IMU, respectively, while Figs. 9 and 10 by sensor 3 and 4, which are the output of the two former sensors added with uniform noise increasing and

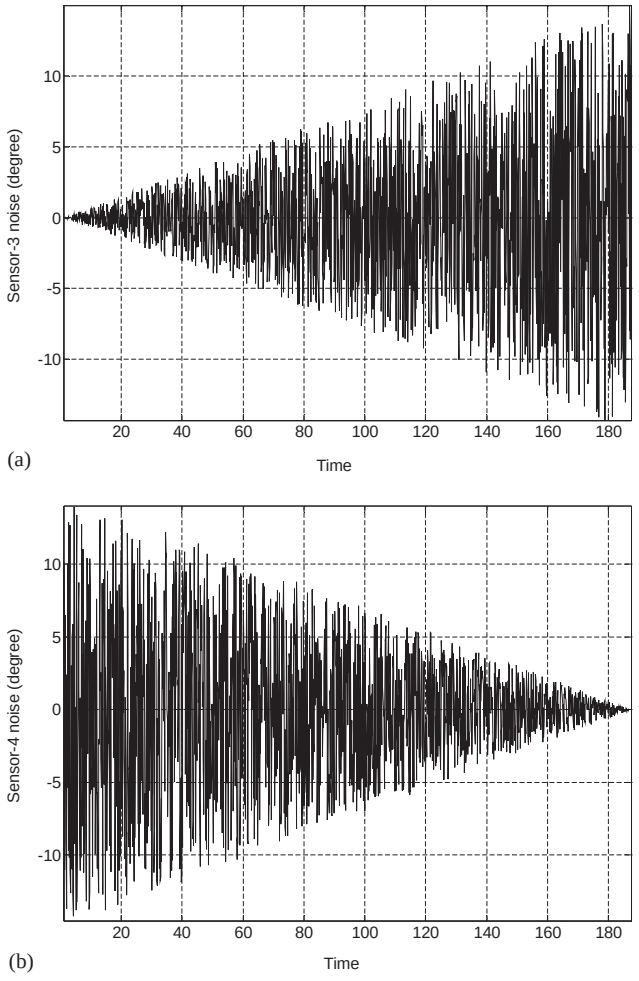

Fig. 6. (a) Added noise profile to the electronic compass data, and (b) to the IMU data.

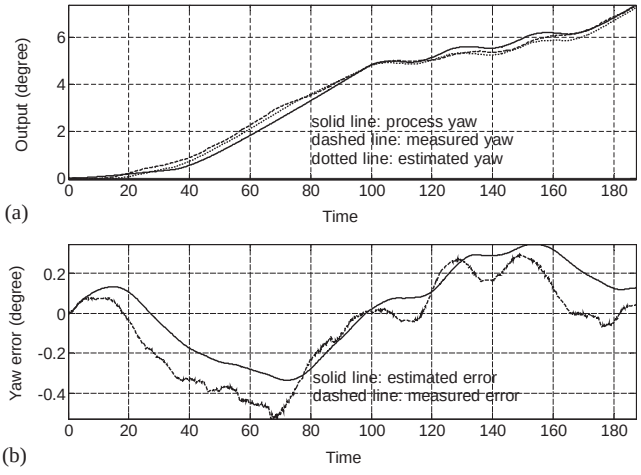

Fig. 7. (a) Process, measured and estimated yaw output, and (b) measured and estimated yaw error of electronic compass.

decreasing with time, respectively. Figs. 7 and 8 show improvements in the level of error produced by the proposed FSKF algorithms as compared to direct

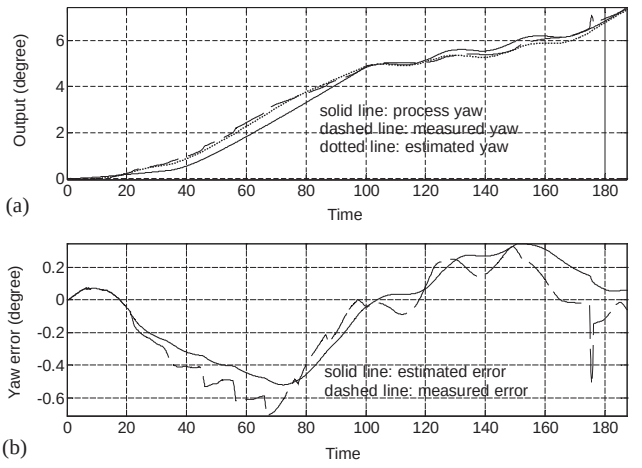

Fig. 8. (a) Process, measured and estimated yaw output, and (b) measured and estimated yaw error of IMU.

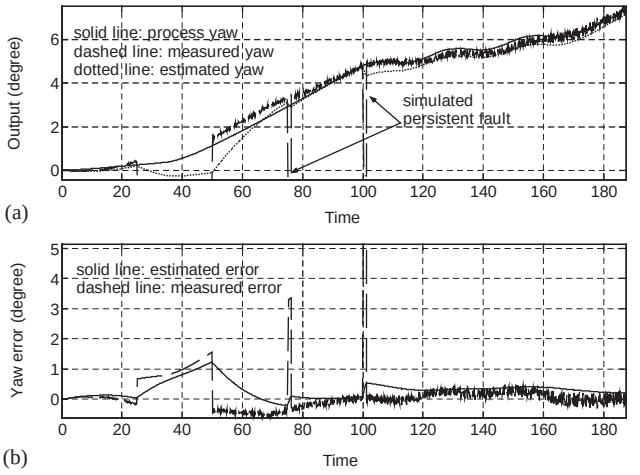

Fig. 9. (a) Process, measured and estimated yaw output, and (b) measured and estimated yaw error of sensor 3 (electronic compass + - simulated noise).

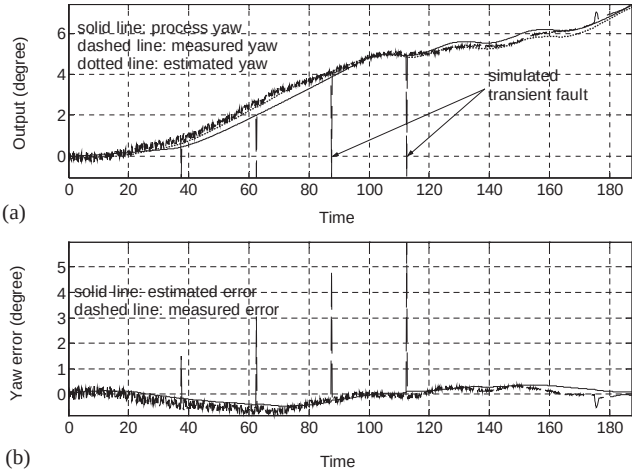

Fig. 10. (a) Process, measured and estimated yaw output, and (b) measured and estimated yaw error of sensor 4 (IMU + simulated noise).

measurements from the sensors. Apart from the improvements in the level of error, Figs. 9 and 10 also show how the proposed algorithms have detected transient and persistent faults in the sensors (see Section 2.2) and made an appropriate recovery.

To fuse the estimated yaw, a centre of gravity method is used

$$\hat{z}_k = \frac{\sum_{i=1}^{n} \hat{z}_{k_i} c_{k_i}}{\sum_{i=1}^{n} c_{k_i}}, \tag{9}$$

where $\hat{z}_{k_i}$ is the output of the ith FSKF ($i = 1, 2, 3, 4$) and c_{k_i} is the respective weight at instant time k. Fig. 11 shows the comparison of the actual and the fused estimated yaw. It is clear, by comparing Fig. 11 and Figs. 7–10 that an improvement has been achieved by fusing the estimated yaw.

Finally, the following performance measure are adopted for comparison purposes:

$$J_{zv} = \sqrt{\frac{1}{n}\sum_{k=1}^{n}(za_k - z_k)^2}, \tag{10}$$

$$J_{ze} = \sqrt{\frac{1}{n}\sum_{k=1}^{n}(za_k - \hat{z}_k)^2}, \tag{11}$$

where za_k is the actual value of the yaw, z_k is the measured yaw, $\hat{z}_k$ is the estimated yaw at an instant of time k and n the number of samples (Table 2).

A close look on the J_{zv} and J_{ze} on Table 2 of each sensor indicates that the FSKF has improved the accuracy of the heading information. The result of fusing the estimated data has shown a further improvement. A slight offset shown by the final fusion result might be caused by an inaccurate model of the process noise (see Appendix A) and its covariance (Q). Adaptation of these parameters is the topic of a future investigation. It should also be noted that from a theoretical point of view, the analysis of the stability of the FSKF needs to be investigated. However, this is not easily undertaken due to the use of the adaptation techniques used herein. Future work will address this issue more rigorously.

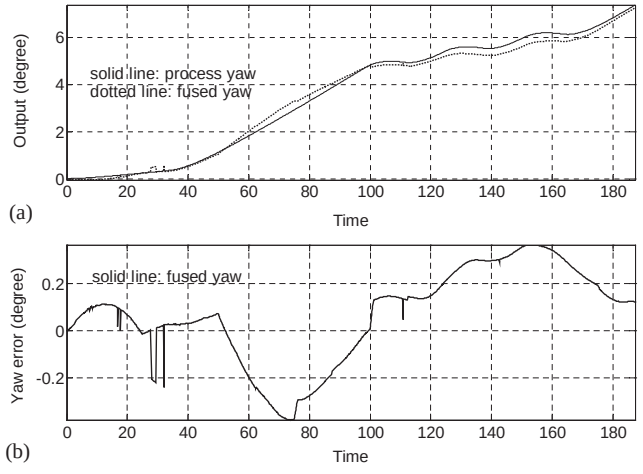

Fig. 11. (a) Process and estimated fused yaw output, and (b) fused yaw error.

Table 2
Comparison of performance

Sensor	Performance	
	J_{zv} (deg)	J_{ze} (deg)
Electronic compass	13.4050	12.1170
IMU	17.3507	15.8216
Electronic compass + noise	37.5725	23.6664
IMU + noise	22.0702	14.6159
Sensor fusion		11.9650

4. Integrated GPS/INS

Here, the fused estimated yaw obtained previously is treated as a single imaginary yaw sensor and used by other INS sensors to transform data from body co-ordinate to Earth co-ordinate frame where integration with GPS data is performed using a combination of fuzzy logic and EKF techniques and can be referred to as FEKF.

A continuous time model of the vehicle motion appropriate to this problem is taken to be

$$\dot{X}(t) = F(X(t)) + W(t), \tag{12}$$

$$Z(t) = H(X(t)) + V(t). \tag{13}$$

Denoted by $X(t) = [\lambda(t)\ \varphi(t)\ \psi(t)\ \vartheta(t)\ \varsigma(t)\ \upsilon(t)]^T$ is the model states. $\lambda(t)$ and $\varphi(t)$ are the longitude and latitude of the AUV position in Earth co-ordinate frame which are obtained from a GPS receiver, $\psi(t)$ is the yaw angle obtained from the imaginary yaw sensor, $\vartheta(t)$ is yaw rate, $\varsigma(t)$ and $\upsilon(t)$ are the surge and sway velocity, respectively.

In this system model, F and H are both continuous functions, continuously differentiable in $X(t)$. The $W(t)$ and $V(t)$ are both zero-mean white noise for the system and measurement models, respectively.

The model states are related through the following kinematically based set of functions ($F(X(t))$ in Eq. (12)):

$$\dot{\varsigma}(t) = 0, \tag{14}$$

$$\dot{\upsilon}(t) = 0, \tag{15}$$

$$\dot{\psi}(t) = \vartheta(t), \tag{16}$$

$$\dot{\vartheta}(t) = 0, \tag{17}$$

$$\dot{\lambda}(t) = \varsigma(t)\cos\psi(t) - \upsilon(t)\sin\psi(t), \tag{18}$$

$$\dot{\varphi}(t) = \varsigma(t)\sin\psi(t) + \upsilon(t)\cos\psi(t). \tag{19}$$

The output measurements are related through the states by the following output matrix:

$$H(X(t)) = \begin{bmatrix} 0 & 0 & 0 & 0 & 1 & 0 \\ 0 & 0 & 0 & 0 & 0 & 1 \\ 0 & 0 & 1 & 0 & 0 & 0 \\ 0 & 0 & 0 & 1 & 0 & 0 \\ 1 & 0 & 0 & 0 & 0 & 0 \\ 0 & 1 & 0 & 0 & 0 & 0 \end{bmatrix}, \tag{20}$$

when GPS signal is available, and when it is not,

$$H(X(t)) = \begin{bmatrix} 0 & 0 & 0 & 0 & 1 & 0 \\ 0 & 0 & 0 & 0 & 0 & 1 \\ 0 & 0 & 1 & 0 & 0 & 0 \\ 0 & 0 & 0 & 1 & 0 & 0 \end{bmatrix}. \tag{21}$$

To obtain an EKF with an effective state prediction equation in a simple form, the continuous time model of (14)–(21) has been linearised about the current state estimates, producing

$$\Phi(t) = \begin{bmatrix} 0 & 0 & 0 & 0 & 0 & 0 \\ 0 & 0 & 0 & 0 & 0 & 0 \\ 0 & 0 & 0 & 1 & 0 & 0 \\ 0 & 0 & 0 & 0 & 0 & 0 \\ 0 & 0 & -\varsigma(t)\sin\psi(t) - \upsilon(t)\cos\psi(t) & 0 & \cos\psi(t) & -\sin\psi(t) \\ 0 & 0 & \varsigma(t)\cos\psi(t) - \upsilon(t)\sin\psi(t) & 0 & \sin\psi(t) & \cos\psi(t) \end{bmatrix} \tag{22}$$

and Γ is a matrix identical as in either (20) or (21). Subsequent discretisation with period $T = 0.125$ s of the linearised model results in an EKF algorithm similar to the SKF algorithms in Appendix A (where Φ and Γ are equivalent to A and H), only this time the Φ matrix is updated at every iteration. The initial conditions are $P_0 = 0.01\ I_6$ and Q is made constant as diag(10, 10, 1, 0.1, 0.1, 0.1). The actual value of R is assumed unknown but its initial value is selected as diag(1000, 1000, 5, 1, 2, 2)

The FSKF algorithm from Section 2 is then implemented, only this time the adaptation of the (i,i)th element of R_k is made in accordance with the (i,i)th element of $delta_k$. Here a single-input–single-output FIS as shown in Fig. 1, is used sequentially to generate the correction factors for the elements in the main diagonal of R_k as the following:

$$R_k(i,i) = R_{k-1}(i,i) + \Delta R_k. \tag{23}$$

Fig. 12 shows the *Hammerhead* AUV trajectory obtained using GPS, dead reckoning using INS sensors (through double integration of the accelerometer data with respect to time) and integrated GPS/INS. As the initial value of R for both $\lambda(t)$ and $\varphi(t)$ is 1000, the standard EKF algorithm puts less weight on the position obtained by GPS and more on the prediction

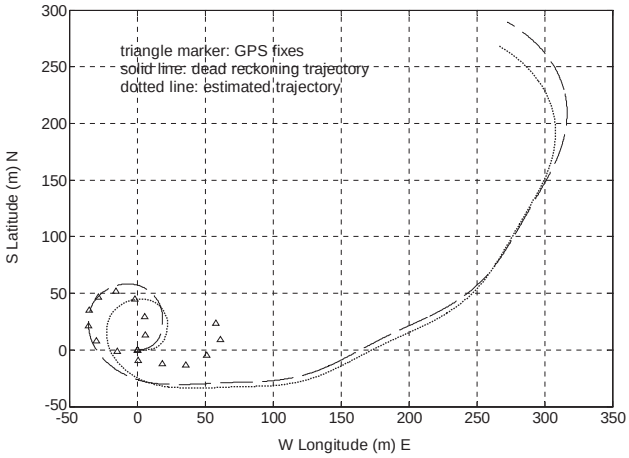

Fig. 12. AUV trajectory obtained using GPS, INS sensors (dead reckoning method) and GPS/INS using EKF without adaptation.

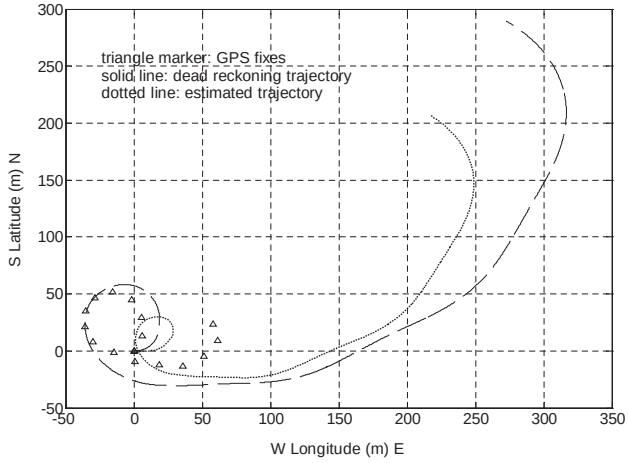

Fig. 13. AUV trajectory obtained using GPS, INS sensors (dead reckoning method) and GPS/INS using EKF with adaptation.

of position obtained from dead reckoning method (using INS sensor data). Fig. 13 shows that the R matrix has been adjusted accordingly and more weight is given to the GPS data, and therefore the estimated trajectory in the integrated INS/GPS is "pulled" a little bit further to the GPS trajectory. However, big discrepancies can still be appreciated between the integrated INS/GPS estimate with respect to the GPS fixes. There are several explanations to this erratic behaviour. The first possibility is that it is caused by the poor level of accuracy of the low-cost GPS being used in this particular application. It is important to note that the proposed algorithm has detected a persistent high actual covariance ($\hat{C}_{Inn_k}$) for both the $\lambda(t)$ and $\varphi(t)$ throughout the trajectory. This results in insufficient weight being given to the GPS fixes in the FEKF and more on the position obtained by the dead reckoning. The second possibility is that the GPS receiver did not lock into a sufficient number of satellites

with a sufficiently small value of position dilution of precision that can provide the required level of accuracy. The use of a differential GPS receiver or a GPS receiver with a wide area augmentation system or a European Geostationary Navigation Overlay Service capability can be considered as a way forward to alleviate this problem.

5. Summary and conclusions

The problem with incomplete a priori knowledge of Q and R is considered. Within this paper, an adaptive Kalman filter approach, based on the filter innovation sequence coupled with fuzzy logic is discussed as an alternative for fusing INS sensor data and integrating INS/GPS position information. Implementation of this approach to the *Hammerhead* heading model, whose responses are measured with electronic compass, IMU and two additional sensors with different noise characteristics, has shown a promising result in improving the estimation of an individual SKF and EKF and enhancing the overall accuracy of the integrated INS/GPS.

Appendix A. Simple Kalman filter algorithms

Given a discrete-time controlled process described by the linear stochastic difference equations:

$$x_{k+1} = A_k x_k + B_k u_k + w_k, \tag{A.1}$$

$$z_k = H_k x_k + v_k, \tag{A.2}$$

where x_k is an $n \times 1$ system state vector, A_k is an $n \times n$ transition matrix, u_k is an $l \times 1$ vector of the input forcing function, B_k is an $n \times l$ matrix, w_k is an $n \times 1$ process noise vector, z_k is an $m \times 1$ measurement vector, H_k is an $m \times n$ measurement matrix and v_k is an $m \times 1$ measurement noise vector. Both the w_k and v_k are assumed to be uncorrelated zero-mean Gaussian white noise sequences with covariance given by

$$E[w_k w_i^T] = \begin{cases} Q_k, & i = k, \\ 0, & i \neq k, \end{cases} \tag{A.3}$$

$$E[v_k v_i^T] = \begin{cases} R_k, & i = k, \\ 0, & i \neq k, \end{cases} \tag{A.4}$$

$$E[w_k v_i^T] = 0, \text{ for all } k \text{ and } i. \tag{A.5}$$

The SKF algorithm can be organised into time update and measurement update equations

Time update equations:

$$\hat{x}_{k+1}^- = A_k \hat{x}_k + B_k u_k, \tag{A.6}$$

$$P_{k+1}^- = A_k P_k A_k^T + Q_k. \tag{A.7}$$

Measurement update equations:

$$K_k = P_k^- H_k^T [H_k P_k^- H_k^T + R_k]^{-1}, \tag{A.8}$$

$$\hat{x}_k = \hat{x}_k^- + K_k [z_k - H_k \hat{x}_k^-], \tag{A.9}$$

$$P_k = [I - K_k H_k] P_k^-. \tag{A.10}$$

The measurement update equations incorporate a new observation into the a priori estimate from the time update equations to obtain an improved a posteriori estimate. In the time and measurement update equations, $\hat{x}_k$ is an estimate of the system state vector x_k, K_k is the Kalman gain and P_k is the covariance matrix of the state estimation error.

References

Asakawa, K., Kojima, J., Kato, Y., Matsumoto, S., & Kato, N. (2000). Autonomous underwater vehicle aqua explorer 2 for inspection of underwater cables. *Proceedings of the 2000 international symposium on underwater technology*, Tokyo, Japan, pp. 242–247.

Chaer, W. S., Bishop, R. H., & Ghough, J. A. (1997). Mixture-of-experts framework for adaptive Kalman filtering. *IEEE Transaction on Systems, Man and Cybernetics—Part B: Cybernetics*, *27*(3), 452–464.

Escamilla-Ambrosio, P. J., & Mort, N. (2001). A hybrid Kalman filter-fuzzy logic multisensor data fusion architecture with fault tolerant characteristics. *Proceedings of the 2001 international conference on artificial intelligence*, Las Vegas, NV, USA, pp. 361–367.

Fitzgerald, R. J. (1971). Divergence of the Kalman filter. *IEEE Transaction on Automatic Control*, *AC-16*(6), 736–747.

Gade, K., & Jalving, B. (1999). An aided navigation post processing filter for detailed seabed mapping UUVs. *Modeling, Identificaion and Control*, *20*(3), 165–176.

Grenon, G., An, P. E., Smith, S. M., & Healey, A. J. (2001). Enhancement of the inertial navigation system for the morpheous autonomous underwater vehicles. *IEEE Journal of Oceanic Engineering*, *26*(4), 548–560.

Hanlon, P. D., & Maybeck, P. S. (2000). Multiple-model adaptive estimation using a residual correlation Kalman filter bank. *IEEE Transaction on Aerospace and Electronic Systems*, *36*(2), 393–406.

Jetto, L., Longhi, S., & Vitali, D. (1999). Localization of a wheeled mobile robot by sensor data fusion based on a fuzzy logic adapted Kalman filter. *Control Engineering Practice*, *7*, 763–771.

Kailath, T. (1968a). An innovations approach to least-squares estimation, Part I: Linear filtering in additive noise. *IEEE Transaction on Automatic Control*, *AC-13*(6), 646–655.

Kailath, T. (1968b). An innovations approach to least-squares estimation, Part II: Linear smoothing in additive white noise. *IEEE Transaction on Automatic Control*, *AC-13*(6), 655–660.

Kailath, T. (1970). The innovations approach to detection and estimation theory. *IEEE Proceedings*, *58*(5), 680–695.

Kinsey, J. C., & Whitcomb, L. L. (2003). Preliminary field experience with the DVLNAV integrated navigation system for manned and unmanned submersibles. *Proceedings of the first IFAC workshop on guidance and control of underwater vehicles*, Newport, South Wales, UK, pp. 83–88.

Kobayashi, K., Cheok, K. C., Watanabe, K., & Muneka, F. (1998). Accurate differential global positioning system via fuzzy logic Kalman filter sensor fusion technique. *IEEE Transactions on Industrial Electronics*, *45*(3), 510–518.

Loebis, D., Chudley, J., & Sutton, R. (2003a). A fuzzy Kalman filter optimized using a genetic algorithm for accurate navigation of an autonomous underwater vehicle. *Proceedings of the sixth IFAC conference on manoeuvring and control of marine craft*, Girona, Spain, pp. 19–24.

Loebis, D., Sutton, R., & Chudley, J. (2002). Review of multisensor data fusion techniques and their application to autonomous underwater vehicle navigation. *Journal of Marine Engineering and Technology*, *A1*, 3–14.

Loebis, D., Sutton, R., & Chudley, J. (2003b). A fuzzy Kalman filter for accurate navigation of an autonomous underwater vehicle. *Proceedings of the first IFAC workshop on guidance and control of underwater vehicles*, Newport, South Wales, UK, pp. 161–166.

Magill, D. T. (1965). Optimal adaptive estimation of sampled stochastic processes. *IEEE Transaction on Automatic Control*, *AC-10*(4), 434–439.

Mehra, R. K. (1970). On the identification of variances and adaptive Kalman filtering. *IEEE Transactions on Automatic Control*, *AC-15*(2), 175–184.

Mehra, R. K. (1971). On-line identification of linear dynamic systems with applications to Kalman filtering. *IEEE Transaction on Automatic Control*, *AC-16*(1), 12–21.

Mohamed, A. H., & Schwarz, K. P. (1999). Adaptive Kalman filtering for INS/GPS. *Journal of Geodesy*, *73*, 193–203.

Størkersen, N., Kristensen, J., Indreeide, A., Seim, J., & Glancy, T. (1998). Hugin—UUV for seabed surveying. *Sea Technology*, *39*(2), 99–104.

Wright, J., Scott, K., Tien-Hsin, C., Lau, B., Lathrop, J., & McCormick, J. (1996). Multi-sensor data fusion for seafloor mapping and ordnance location. *Proceedings of the 1996 symposium on autonomous underwater vehicle technology*, Monterey, CA, USA, pp. 167–175.

Yun, X., Bachmann, R. E., McGhee, R. B., Whalen, R. H., Roberts, R. L., Knapp, R. G., Healey A, J., & Zyda, M. J. (1999). Testing and evaluation of an integrated GPS/INS system for small AUV navigation. *IEEE Journal of Oceanic Engineering*, *24*(3), 396–404.